BJP British Journal of Pharmacology

DOI:10.1111/bph.13246
www.brjpharmacol.org

RESEARCH PAPER

A polyspecific drug/proton antiporter mediates diphenhydramine and clonidine transport at the mouse blood-retinal barrier

Hélène Chapy[1,2,3]*, Pascal André[1,2,3]*, Xavier Declèves[1,2,3,4], Jean-Michel Scherrmann[1,2,3,4] and Salvatore Cisternino[1,2,3,4]

[1]*Variabilité de réponse aux psychotropes, INSERM U1144, Paris, France,* [2]*UMR-S 1144, Université Paris Descartes, Paris, France,* [3]*UMR-S 1144, Université Paris Diderot, Paris, France, and* [4]*Pharmacokinetics, Assistance Publique des Hôpitaux de Paris – AP-HP, Paris, France*

Correspondence
Salvatore Cisternino, INSERM UMR-S1144, Université Paris Descartes, Faculté de Pharmacie, Laboratoire de pharmacocinétique, 4, Avenue de l'Observatoire, 75006 Paris, France. E-mail: salvatore.cisternino@aphp.fr

*These authors contributed equally to this work.

Received
26 March 2015
Revised
11 June 2015
Accepted
3 July 2015

BACKGROUND AND PURPOSE

Transporters at the blood-retinal barrier (BRB), as at the blood–brain barrier (BBB), regulate the distribution of compounds into the neural parenchyma. However, the expression of BRB transporters and their quantitative impact *in vivo* are still poorly understood.

EXPERIMENTAL APPROACH

Clonidine and diphenhydramine are substrates of a novel BBB drug/proton-antiporter. We evaluated their transport at the BRB by *in situ* carotid perfusion in wild-type or knocked-out mice for Oct1-3 (Slc22a1-3).

KEY RESULTS

At pharmacological exposure levels, carrier-mediated BRB influx was 2 and 12 times greater than the passive diffusion rate for clonidine and diphenhydramine, respectively. Functional identification demonstrated the involvement of a high-capacity potassium- and sodium-independent proton-antiporter that shared the features of the previously characterized clonidine, diphenhydramine and cocaine BBB transporter. The functional characterization suggests that SLC transporters Oct1-3, Mate1 (Slc47a1) and Octn1-2 (Slc22a4-5) are not involved. Melanin/retinal toxic drugs like antimalarials (amodiaquine, quinine), quinidine and tricyclic antidepressants (imipramine) acted as inhibitors of this proton-antiporter. The endogenous indole derivative tryptamine inhibited the transporter, unlike 5-HT (serotonin), dopamine or L-DOPA. *Trans*-stimulation experiments with [^{3}H]-clonidine at the BRB indicated that diphenhydramine, nicotine, oxycodone, naloxone, tramadol, 3,4-methylenedioxyamphetamine (MDMA, ecstasy), heroin, methadone and verapamil are common substrates.

CONCLUSIONS AND IMPLICATIONS

A proton-antiporter is physiologically involved in the transport of clonidine and diphenhydramine and is quantitatively more important than their passive diffusion flux at the mouse BRB. The features of this molecularly unidentified transporter highlight its importance in regulating drug delivery at the retina and suggest that it has the capacity to handle several drugs.

Abbreviations

ACTZ, acetazolamide; BBB, blood–brain barrier; BRB, blood-retina barrier; CA, carbonic anhydrase; DPH, diphenhydramine; iBRB, inner blood-retina barrier; KO, knockout; MDMA, 3,4-methylenedioxyamphetamine (ecstasy); NMDG, N-methyl D-glucamine; oBRB, outer blood-retina barrier; P-gp, P-glycoprotein; PD, pharmacodynamics; PK, pharmacokinetics; RPE, retinal pigment epithelial cells; TKO, triple knockout (Abcb1a$^{-/-}$, Abcb1b$^{-/-}$, Abcg2$^{-/-}$) mice; WT, wild-type mice

Tables of Links

TARGETS
ABCB1
ABCG2
MATE1 (SLC47A1)
OCT1-3 (SLC22A1-3)
OCTN1-2 (SLC22A4-5)

LIGANDS		
5-HT	Dopamine	Nicotine
Acetazolamide	Guanidine	Oxycodone
Carnitine	Histamine	Quinidine
Choline	Imipramine	Quinine
Clonidine	L-DOPA	Sucrose
Cocaine	MDMA	TEA
Corticosterone	Methadone	Tryptamine
Desipramine	Morphine	Verapamil
Diphenhydramine	Naloxone	

These Tables list key protein targets and ligands in this article which are hyperlinked to corresponding entries in http://www.guidetopharmacology.org, the common portal for data from the IUPHAR/BPS Guide to PHARMACOLOGY (Pawson *et al.*, 2014) and are permanently archived in the Concise Guide to PHARMACOLOGY 2013/14 (Alexander *et al.*, 2013).

Introduction

The expression of xenobiotic transporters at certain critical blood-tissue interfaces, also known as barriers, reinforces their role in regulating the passage of specific drugs across tight endothelial and epithelial surfaces (Abbott *et al.*, 2010; Giacomini *et al.*, 2010). Like the tightly apposed brain endothelial cells that form the blood–brain barrier (BBB), the 'inner' blood-retinal barrier (iBRB) is composed of a few intra-retinal capillary endothelial cells that control the access of compounds to the retinal neural tissue. The second retinal barrier, also called the 'outer' blood-retinal barrier (oBRB) and which covers the entire retina, is formed by the tight retinal pigment epithelium (RPE). The oBRB separates the fenestrated choroid capillaries on its basolateral side from the neural retina on its apical side, and represents the most important BRB in term of surface and biochemical nutrient delivery (Newman, 2013). Although, the pharmacokinetic (PK) properties of the BRB have mainly been explored in diverse cell lines, their functions *in vivo* have been poorly addressed.

Due to their protective function and relatively early discovery, the role of the unidirectional xenobiotic efflux or ATP-binding cassette (ABC) transporters, such as P-glycoprotein (P-gp/ABCB1a), has been investigated considerably more than that of bidirectional drug transporters from the solute carrier superfamily (SLC). However, SLC drug transporters could contribute to both the pharmacodynamic (PD) and toxicological aspects of drugs/substrates (Giacomini *et al.*, 2010; Ronaldson and Davis, 2013). Clonidine, an α_2-adrenoreceptor agonist and valuable antihypertensive and for the treatment of neurodegenerative processes at the retina (Crassous *et al.*, 2007), and diphenhydramine (DPH), a widely used drug beneficial in diverse allergy manifestations, constitute two known prototypical substrates for the characterization of a novel drug/proton antiporter that is still unknown at the molecular level (Fischer *et al.*, 2006; Andre *et al.*, 2009; Sadiq *et al.*, 2011). Although the functional characterization of this drug/proton-antiporter *in vitro* in brain and retinal endothelial cell lines, as well as in intestinal and retinal epithelial cell lines, has been carried out by several groups (Han *et al.*, 2001; Fischer *et al.*, 2006; Zhang *et al.*, 2006; Okura *et al.*, 2008; Chapy *et al.*, 2014; Kubo *et al.*, 2014), its *in vivo* biochemical and functional features, showing that clonidine and DPH are common substrates of a single proton-antiporter (Andre *et al.*, 2009), have only been reported at the mouse BBB. Indeed, one difficulty in specifically assessing the function of this transporter by systemic administration of inhibitors *in vivo* is due to the lack of compounds capable of reaching the concentration necessary to inhibit its function.

The physiological expression of BBB or BRB transporters supports their tissue-specific biochemical properties, such as specific nutrient transport and/or compound removal (Andre *et al.*, 2012). This expression pattern forms the basis of their diversity of tissue functions, like their molecular trafficking properties. To obtain further biochemical and pharmacological insights into the physiological role of this molecularly unidentified transporter in specific or shared mechanisms at these blood-neural barriers, we assessed clonidine and DPH transport by *in situ* carotid perfusion, under conditions of concentration and exposure time selected to specifically measure initial transport at the BRB (Cattelotte *et al.*, 2008; Andre *et al.*, 2009; 2012).

This *in vivo*/*in situ* model permits the functional identity and quantitative properties of transport to be determined,

and can be used to evaluate and identify the contribution of carrier-mediated systems including those with high capacity, by assessing the concentration-dependence of the transport using drug concentrations high enough to surpass the K_m of the transporter (Kell *et al.*, 2013). Our results show that the transport of clonidine and DPH at the mouse BRB involves a common carrier-mediated system functionally identified as a sodium-independent proton/drug-antiporter, in addition to a relative minor passive diffusion component. The features of this molecularly unidentified transporter highlight its importance in governing clonidine and DPH delivery at the retina.

Methods

Animals

Swiss and Fvb male mice (25–35 g, 7–11 weeks old) were obtained from Janvier (Genest, France). The Fvb mice triple knockout (TKO) P-gp and Bcrp (Abcb1a$^{-/-}$, Abcb1b$^{-/-}$, Abcg2$^{-/-}$), the Fvb double KO for Oct1 and Oct2 (Oct1$^{-/-}$, Oct2$^{-/-}$) and the Fvb KO for Oct3$^{-/-}$ mice were bred in house from progenitors obtained from the laboratory of Dr. Alfred H. Schinkel (The Netherlands Cancer Institute, Amsterdam, the Netherlands). The 650 mice were housed in a controlled environment (22°C ± 2°C; 55% humidity ± 10% relative humidity) and a 12 h dark–light cycle, with access to food and tap water *ad libitum*. All studies involving animals are reported in accordance with the ARRIVE guidelines for reporting experiments involving animals (Kilkenny *et al.*, 2010; McGrath *et al.*, 2010). and complied with the ethical rules of the European directive (2010/63/EU) for experimentation with laboratory animals; they were approved by the ethics review committee of Paris Descartes University (study approval n°12–183/12–2012).

Drugs and chemicals

[^{3}H]-clonidine (2.6×10^{12} Bq·mmol^{-1}), [^{14}C]-sucrose (2×10^{10} Bq·mmol^{-1}) and [^{3}H]-histamine (52×10^{10} Bq·mmol^{-1}) were purchased from Perkin Elmer (Courtaboeuf, France). [^{14}C]-diphenhydramine (26×10^{10} Bq·mmol^{-1}) was purchased from Moravek (La Brea, CA, USA) and unlabelled DPH was purchased from Inresa (Strasbourg, France). 3,4-Methylenedioxyamphetamine (MDMA; purity > 99%) was synthesized by chemistry departments of Paris Descartes University (Dr Galons). Elacridar (GF120918) was kindly provided by GlaxoSmithKline (Collegeville, PA, USA). All other chemicals were purchased from Sigma (Saint Quentin-Fallavier, France).

In situ *carotid perfusion*

Surgical procedure and perfusion. The transport of [^{3}H]-clonidine and [^{14}C]-DPH was measured by *in situ* carotid perfusion (Cattelotte *et al.*, 2008). Mice were anaesthetized with ketamine-xylazine (140-8 mg·kg^{-1}, i.p.) and a catheter was inserted into the right carotid artery. The perfusion liquid was connected to the catheter. Before perfusion, the thorax was opened and the heart was cut. Perfusion was started immediately at a flow rate of 2.5 mL·min^{-1}. Each mouse was perfused with [^{3}H]-clonidine (11×10^3 Bq·mL^{-1}; ~9 nmol·L^{-1}) and [^{14}C]-sucrose (4.10^3 Bq·mL^{-1}) as a vascular marker or with [^{14}C]-DPH (4×10^3 Bq·mL^{-1}; ~1.4 µmol·L^{-1}) and [^{3}H]-histamine (11×10^3 Bq·mL^{-1}; vascular marker). Perfusion with [^{3}H]-clonidine was terminated after 120 s by decapitating the mouse and 60 s with [^{14}C]-DPH. The right eye (without optic nerve) was removed from the skull and dissected out on a freezer pack. The anterior and posterior segments and vitreous humour of the eye were dissected out in some experiments. Tissues samples and aliquots of perfusion fluid were placed in preweighed vials and weighed, digested with Solvable (Perkin Elmer) and mixed with Ultima-gold XR (Perkin Elmer). Dual label disintegration per minute (dpm) counting was carried out in a Tri-Carb 2810TR (Perkin Elmer).

Perfusion fluid. The perfusion fluid was Krebs carbonate-buffered physiological saline (mmol·L^{-1}): 128 NaCl, 24 $NaHCO_3$, 4.2 KCl, 2.4 NaH_2PO_4, 1.5 $CaCl_2$, 0.9 $MgSO_4$ and 9 D-glucose, unless otherwise specified. The perfusion fluid was warmed to 37°C in a water bath and gassed with 95% O_2/5% CO_2 to bring pH to 7.40, unless otherwise specified. In some experiments hydrochloric acid was added to the gassed perfusion fluid, to bring the pH of the perfusion fluid to 5.40, or 6.40. NH_4Cl (30 mmol·L^{-1}) was added in the perfusion fluid to modify intracellular pH (pH_i). Krebs carbonate perfusate was changed to remove some ionorganic ions by iso-osmotic replacement. Chloride-free perfusion fluid contained gluconate and nitrate. Sodium was replaced by potassium in the 'K^+' perfusion fluid (K^+ 154 mmol·L^{-1}), by lithium chloride in the 'Li^+' fluid (Li^+ 128 mmol·L^{-1}), by mannitol in the 'mannitol' fluid (mannitol 256 mmol·L^{-1}, Cl^- 3 mmol·L^{-1}), and by N-methyl D-glucamine chloride in the NMDG-Cl (128 mmol·L^{-1}) fluid. Mice were also perfused with HEPES-buffered saline (mmol·L^{-1}): 152 NaCl, 4.2 KCl, 1.5 $CaCl_2$, 0.9 $MgSO_4$, 10 HEPES and 9 D-glucose, warmed to 37°C, gassed with O_2 and brought to pH 7.40 with sodium hydroxide. The perfusion fluid that controlled the extracellular vascular pH (pH_e) was always adjusted and checked with a digital pH meter (±0.05 pH units) immediately before perfusion.

[^{3}H]-clonidine and [^{14}C]-DPH transport study conditions. Initial transport rates were measured under *trans*-influx zero conditions by perfusing [^{3}H]-clonidine for 120 s and [^{14}C]-DPH for 60 s. The perfusion time adopted ensured that the eye distribution of the drug was that of the initial linear part of the distribution kinetics (data not shown). So, the apparent distribution in the eye did not reach (pseudo-) equilibrium during this initial linear phase. The luminal (blood side) membrane is the only kinetic interface that affected the distribution of radiolabelled clonidine or DPH. *Cis*-inhibition was performed by co-perfusion of the radiolabelled compounds with the selected unlabelled drug. *Trans*-stimulation of the distribution of [^{3}H]-clonidine in the eye was performed using two syringes, each in its own infusion pump, and connected to the carotid catheter by a four-way valve. This enabled immediate switching from one syringe to the other. The tissue was first 'loaded' by perfusion with [^{3}H]-clonidine (~9 nmol·L^{-1}) in Krebs carbonate buffer (pH_e 7.40) for 120 s. The second perfusion (pH_e 6.40) was with [^{14}C]-sucrose (4×10^3 Bq·mL^{-1}), with or without the unlabelled test compound for 60 s.

Apparent tissue distribution volume and initial transport parameters. Calculations were done as previously described (Takasato *et al.*, 1984; Cattelotte *et al.*, 2008; Andre *et al.*,

2012). The eye 'vascular' volume was estimated using the vascular marker distribution volume (V_v; $\mu L \cdot g^{-1}$):

$$V_v = \frac{X^*}{C^*_{perf}} \quad (1)$$

where X^* ($dpm \cdot g^{-1}$) is the amount of the vascular marker in the tissue sample and C^*_{perf} ($dpm \cdot \mu L^{-1}$) its concentration in the perfusion fluid. The data for any mouse whose V_v was above the normal value (Cattelotte *et al.*, 2008) was excluded from the study.

The apparent tissue distribution volume (V_{eye}, $\mu L \cdot g^{-1}$) was calculated as

$$V_{eye} = \frac{X_{tissue}}{C_{perf}} \quad (2)$$

where X_{tissue} ($dpm \cdot g^{-1}$) is the calculated amount of [^{3}H]-clonidine or [^{14}C]-DPH from the right eye and C_{perf} ($dpm \cdot \mu L^{-1}$) its concentration in the perfusion fluid. This total activity was corrected for 'vascular' contamination using the V_v subtraction:

$$X_{tissue} = X_{tot} - V_v C_{perf} \quad (3)$$

where X_{tot} ($dpm \cdot g^{-1}$) is the total quantity of [^{3}H]-clonidine or [^{14}C]-DPH measured in the sample tissue.

As the vascular space was 'washed' in the final perfusion with [^{3}H]-clonidine-free fluid in the *trans*-stimulation experiments, there was no need to subtract the [^{3}H]-clonidine vascular content. The [^{14}C]-sucrose perfused during the final wash-out procedure was only used to estimate the V_v for checking barriers integrity during these experiments.

The initial transport expressed as a K_{in} ($\mu L \cdot s^{-1} \cdot g^{-1}$) was calculated from

$$K_{in} = \frac{V_{eye}}{T} \quad (4)$$

where T is the perfusion time (s).

The permeability-surface area product (PS, $\mu L \cdot s^{-1} \cdot g^{-1}$) was calculated.

$$PS = -F \ln(1 - K_{in}/F) \quad (5)$$

where F (vascular fluid flow rate; 19.2 $\mu L \cdot s^{-1} \cdot g^{-1}$) has been previously measured with [^{3}H]-diazepam, a free passively diffusible totally extracted compound (Takasato *et al.*, 1984; Cattelotte *et al.*, 2008; Andre *et al.*, 2012).

The retina flux (J_{in}; $nmol \cdot s^{-1} \cdot g^{-1}$) is given by:

$$J_{in} = PS \times C_{tot} \quad (6)$$

The clonidine and DPH retinal flux (J_{in}) is described as having saturable (Michaelis–Menten term) and a passive unsaturable components:

$$J_{in} = \frac{V_{max} C_{tot}}{K_m + C_{tot}} + K_{passive} C_{tot} \quad (7)$$

where C_{tot} ($mmol \cdot L^{-1}$) is the total clonidine or DPH concentration in the perfusate, V_{max} ($nmol \cdot s^{-1} \cdot g^{-1}$) is the maximal velocity of transport, K_m ($mmol \cdot L^{-1}$) represents the concentration at the half-maximal carrier velocity. $K_{passive}$ ($\mu L \cdot s^{-1} \cdot g^{-1}$) is an unsaturable component, which represents the rate of transport by passive diffusion. The data were fitted using non-linear regression analysis.

A relative value for the permeability of a compound into the tissue was obtained from the extraction parameter (E, %), calculated as:

$$E = \frac{K_{in}}{F} \cdot 100 \quad (8)$$

Data analysis

Data are presented as means ± SD. One-way ANOVA and *post hoc* test (Dunnett) or Student's two-tailed unpaired *t*-test were used to identify significant differences and statistical significance was set at $P < 0.05$. The transport parameters (K_m, V_{max}, $K_{passive}$) were estimated by plotting drug flux data against total concentration using Eq. 7 and non-linear regression with WinNonlin® software (Pharsight, Certara, Princeton, NJ, USA). The errors associated with these parameters are asymptotic standard errors returned by the non-linear regression routine.

Results

[^{3}H]-clonidine transport at the luminal/vascular membrane side of the eye barriers

We evaluated the kinetic contributions of the anterior and posterior (e.g. retina) eye barriers by measuring the [^{3}H]-clonidine (11×10^3 $Bq \cdot mL^{-1}$) distribution, corrected by the [^{14}C]-sucrose space, after 120 s of carotid perfusion. The anterior and posterior barriers and the vitreous humour were obtained by eye dissection. The accumulation of [^{3}H]-clonidine in the vitreous humour was too low to measure, so that it made no contribution to the distribution of [^{3}H]-clonidine between the anterior and posterior regions of the eye. [^{3}H]-clonidine distribution volume in the posterior eye region, which includes the retina, the choroid and the sclera, accounted for 87 ± 6% (n = 5) of the total [^{3}H]-clonidine distribution volume in the eye, corrected for the [^{14}C]-sucrose space. [^{3}H]-clonidine distribution volume measured for the whole eye mainly reflected the transport at the BRB interfaces because the anterior eye region accounted for only ~13% of the total [^{3}H]-clonidine eye distribution. In order to avoid variations in tissue samples due to manual dissection, the whole eye was used to measure [^{3}H]-clonidine accumulation and for a similar reason [^{14}C]-DPH, which in these conditions mainly reflects transport across the posterior/retina BRB.

Passive and carrier-mediated clonidine and DPH transport components at the retina

Concentration dependence of clonidine transport. The retina flux (J_{in}) of clonidine (Figure 1A) was measured at multiple clonidine concentrations in Krebs carbonate buffer (pH_e 7.40) for 120 s, by carotid perfusion. The total flux from which the unsaturated flux was subtracted, gave the carrier-mediated flux that was plotted against the total compound concentration. The regression plot of the carrier-mediated flux was best fitted with a Hill coefficient of 1. The eye carrier-mediated flux model gave an apparent K_m of 0.57 ± 0.16 $mmol \cdot L^{-1}$ and

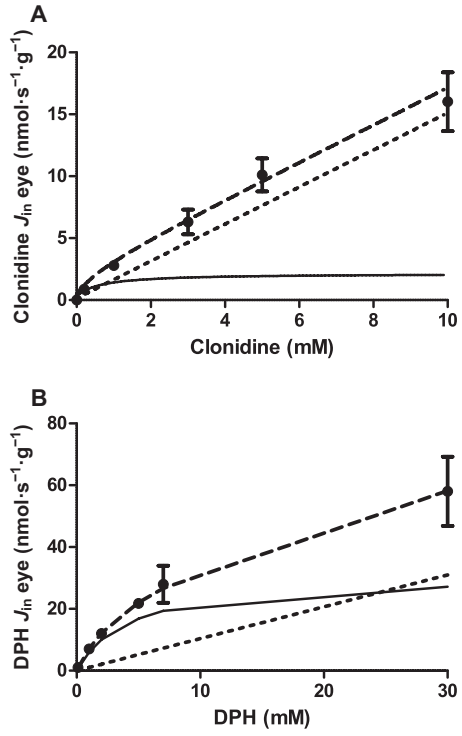

Figure 1

Total flux (J_{in}; nmol·s^{-1}·g^{-1}; dashed line) reported as mean ± SD measured in the mouse right eye (n = 5–7 per concentration) and fitted to total clonidine (A) or DPH (B) concentrations in Krebs carbonate perfusion fluid at pH$_e$ 7.40. The straight dotted line (A, B) represents the passive diffusion flux for clonidine or DPH (cationic and neutral forms). The solid line (A, B) represents data fitted to the carrier-mediated Michaelis–Menten equation by non-linear least-squares regression obtained by subtracting the passive flux from the total flux. The estimated parameters for BRB clonidine transport are: K_m = 0.57 ± 0.16 mmol·L^{-1}, V_{max} = 2.35 ± 0.67 nmol·s^{-1}·g^{-1}, $K_{passive}$ = 1.49 ± 0.17 µL·s^{-1}·g^{-1}. The estimated parameters for BRB DPH transport are K_m = 4.18 ± 0.49 mmol·L^{-1}, V_{max} = 30.95 ± 3.04 nmol·s^{-1}·g^{-1}, $K_{passive}$ = 1.03 ± 0.10 µL·s^{-1}·g^{-1}.

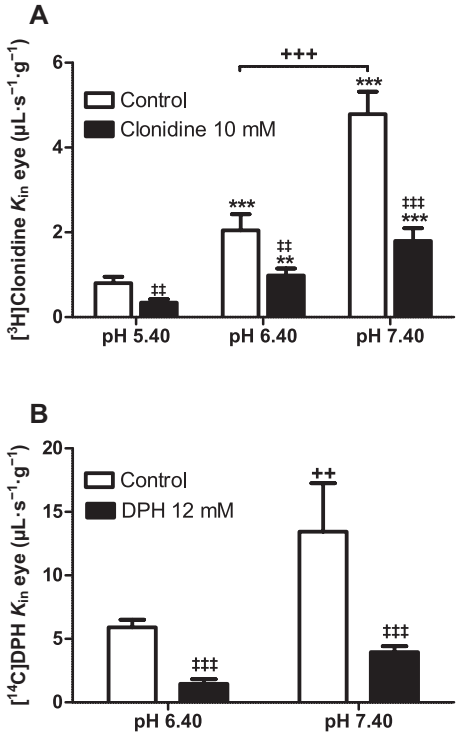

Figure 2

Effect of the Krebs carbonate perfusion fluid pH$_e$ (5.40, 6.40 or 7.40) on the BRB transport of [^{3}H]-clonidine (A) or [^{14}C]-DPH (B) (K_{in}; µL·s^{-1}·g^{-1}) measured at the BRB by *in situ* mouse carotid perfusion for 120 s (clonidine) or 60 s (diphenhydramine; DPH) with or without (control) coperfusion with unlabelled clonidine (10 mmol·L^{-1}; A) or DPH (12 mmol·L^{-1}; B). Data indicate means ± SD of 5–7 mice. $^{**}P$ < 0.01, $^{***}P$ < 0.001 compared with or without the addition of unlabelled clonidine (10 mmol·L^{-1}) at pH$_e$ 5.40. ^{++}P < 0.01, ^{+++}P < 0.001 for comparisons of pH$_e$ 7.40 to pH$_e$ 6.40 values without added clonidine (10 mmol·L^{-1}) or DPH (12 mmol·L^{-1}). ‡‡P < 0.01, ‡‡‡P < 0.001 for comparisons of data obtained at the same pH$_e$ with or without added clonidine (10 mmol·L^{-1}) or DPH (12 mmol·L^{-1}).

a V_{max} of 2.35 ± 0.67 nmol·s^{-1}·g^{-1} for clonidine (Figure 1A). The total (cationic and neutral forms) eye passive diffusion component at pH 7.40 gave a $K_{passive}$ of 1.49 ± 0.17 µL·s^{-1}·g^{-1} for clonidine, equivalent to an extraction $E_{passive,eye}$ of 7.8%. The eye transport rate (K_{in}) under unsaturated conditions (clonidine concentration <K_m) was 5.1 ± 0.6 µL·s^{-1}·g^{-1}, which corresponded to an $E_{total,eye}$ extraction of 26.6% for clonidine. A comparison of the *in vivo* passive (~1.49 µL·s^{-1}·g^{-1}) and carrier-mediated (~3.6 µL·s^{-1}·g^{-1}) transport rates at pH$_e$ 7.40 suggests that the carrier-mediated influx of clonidine is 2.1 times greater than its passive diffusion when concentrations are less than the apparent carrier-mediated K_m. Total pharmacological concentrations of clonidine in the plasma of rodents and humans are reported to be lower than 20 nmol·L^{-1} (Pomerleau *et al.*, 2014), matching the linear/proportional kinetics (first order kinetics; unbound concentration < K_m) of the transporter.

The previously reported brain transport rate (K_{in}) for clonidine under unsaturated conditions was 6.1 ± 0.6 µL·s^{-1}·g^{-1} ($E_{total,brain}$ 14.2%; Andre *et al.*, 2009). In the brain, the extraction $E_{passive,brain}$, for clonidine was 6.5% (Andre *et al.*, 2009). The passive diffusion rate or extraction of the cationic form of clonidine was estimated from the saturated eye transport component measured at pH$_e$ 5.40, where clonidine is only cationic ($K_{passive,cationic}$ 0.3 µL·s^{-1}·g^{-1}; Figure 2). The extraction of the cationic clonidine form by passive diffusion in the eye ($E_{passive,cationic,eye}$) was 1.6% and that of the brain ($E_{passive,cationic,brain}$) was 1.8% (Andre *et al.*, 2009).

Concentration-dependence of DPH transport. The retina flux (J_{in}) of diphenhydramine (Figure 1B) was measured by carotid perfusion (60 s) in Krebs carbonate buffer (pH$_e$ 7.40) at multiple DPH concentrations. The total flux, from which the unsaturated flux was subtracted, gave the carrier-mediated flux that was plotted against the total compound concentration. The regression plot of the carrier-mediated flux was best fitted with a Hill coefficient of 1. The eye carrier-mediated flux model gave an apparent K_m of 4.18 ± 0.49 mmol·L^{-1} and a V_{max} of 30.95 ± 3.04 nmol·s^{-1}·g^{-1} for DPH (Figure 1B). The total (cationic and neutral forms) eye passive diffusion

component at pH 7.40 gave a $K_{passive}$ of 1.03 ± 0.10 µL·s^{-1}·g^{-1} for DPH, equivalent to an extraction $E_{passive,eye}$ of 5.4%. A comparison of the *in vivo* passive (~1.03 µL·s^{-1}·g^{-1}) and carrier-mediated (~12.5 µL·s^{-1}·g^{-1}) transport rates suggests that the BRB carrier-mediated influx of DPH is 12.1 times greater than its passive diffusion when concentrations are less than the apparent carrier-mediated K_m. Total pharmaco-toxicological concentrations of DPH in the plasma of rodents and humans are reported to be lower than 40 µmol·L^{-1} (Pragst *et al.*, 2006) matching the linear/proportional kinetics (first-order kinetics; unbound concentration < K_m) of the transporter.

Effects of inorganic ions on [^{3}H]-clonidine BRB transport

To gain further biochemical information in order to better assess its functional identity, the intracellular pH (pH_i) and the extracellular proton (pH_e), sodium, potassium or chloride concentrations were manipulated in several experiments.

Modulations of the extracellular/vascular pH (pH_e). The proportion of neutral and cationic species of clonidine and DPH depends on the pH_e, which can be estimated using a basic pK_a value of 8.21 and 8.98 in water, respectively. Clonidine is 0.15% neutral at pH_e 5.40, 1.5% at pH_e 6.40 and 13.4% at pH_e 7.40. DPH is 0.26% neutral at pH_e 6.40 and 2.6% at pH_e 7.40. The transport (K_{in}) of [^{3}H]-clonidine measured without adding unlabelled clonidine increased significantly (159%) between pH_e 5.40 and 6.40, whereas the amount of uncharged clonidine was not significantly increased (<1%). It also increased by 119% between pH_e 6.40 and 7.40 (Figure 2A). Adding unlabelled clonidine (10 mmol·L^{-1}) significantly decreased by 2.4-, 2.1- and 2.7-fold the [^{3}H]-clonidine BRB transport at pH 5.40, 6.40 and 7.40, respectively, suggesting that a saturable carrier-mediated system was involved (Figure 2A). The transport (K_{in}) of [^{14}C]-DPH measured without adding unlabelled DPH increased significantly (210%) between pH_e 6.40 and 7.40 (Figure 2B). Adding unlabelled DPH (12 mmol·L^{-1}) significantly decreased the [^{14}C]-DPH K_{in} eye transport at pH 6.40 and 7.40, respectively, by 4.1- and 3.1-fold, suggesting the involvement of a saturable carrier-mediated system (Figure 2B). These inhibition effects by unlabelled clonidine or DPH shown at pH_e 5.40 or 6.40 could suggest that the cationic form (>98%) is a substrate of the transporter. However, with these functional approaches we cannot reject that the neutral form of clonidine or DPH is not a substrate.

Alteration of the intracellular pH (pH_i). To limit the confounding effect of the proportion of neutral clonidine and DPH in the extracellular/vascular compartment and thus to illustrate better the effect of proton on the transporter activity, [^{3}H]-clonidine transport (pH_e 7.40) was also evaluated with protocols that increased or decreased the pH_i, and [^{14}C]-DPH with a protocol that increased pH_i.

Alkalinization protocols. NH_4Cl affects the intracellular pH (pH_i) by releasing free NH_3 that enters cells and increase pH_i. [^{3}H]-Clonidine or [^{14}C]-DPH was perfused in Krebs carbonate fluid with or without NH_4Cl (30 mmol·L^{-1}) adjusted to pH_e 7.40. This significantly reduced 2.5- and 2.8-fold the BRB transport of [^{3}H]-clonidine and [^{14}C]-DPH respectively (Figure 3A,B).

Physiologically, the vascular barrier cells are exposed to the blood, which is a carbonate buffer. Replacing abruptly the vascular carbonate-buffer (e.g. blood) with a carbonate-free fluid lead to an abrupt rapid increase in pH_i (Taylor *et al.*, 2006). The [^{3}H]-clonidine transport with carbonate-free HEPES fluid (pH_e 7.40) was significantly 1.7-fold reduced compared with the transport measured after perfusion with Krebs carbonate fluid (pH_e 7.40; Figure 3A). This 'carbonate/no carbonate' change was partially reduced when acetazolamide (ACTZ; 10 mmol·L^{-1}), a permeating carbonic anhydrase (CA) inhibitor, was added to the HEPES-buffered fluid (pH_e 7.40; Figure 3A) in accordance with the expected CA-sensitive process in this pH_i alteration mechanism (Ochrietor *et al.*, 2005; Taylor *et al.*, 2006; Andre *et al.*, 2009). The transport of [^{3}H]-clonidine in Krebs carbonate buffer (pH_e 7.40) containing different amounts of HEPES (5–25 mmol·L^{-1}) was unaffected, suggesting that HEPES had no direct effect on [^{3}H]-clonidine transport (data not shown).

Acidification protocol. Sodium depletion in the vascular/extracellular space cannot be used to obtain acute acidification at the BRB, in contrast to the BBB. In order to generate an abrupt decrease in pH_i, we therefore used the butyrate protocol, which consists of perfusion with Krebs carbonate fluid (pH_e 7.40) in which chloride is replaced by butyrate (100 mmol·L^{-1}). This protocol resulted in pH_i acidification in certain cell types that are capable of mediating efficient butyrate transport through a proton-symporter (e.g. RPE/oBRB). The acidifying effect of butyrate on cells also depends on the duration of its incubation and the pH of the extracellular medium (Kenyon *et al.*, 1997; Kuwayama *et al.*, 2008). Here, mice were perfused with [^{3}H]-clonidine in Krebs carbonate fluid with or without butyrate (100 mmol·L^{-1}), adjusted to pH_e 7.40. The resulting drop in the pH_i of the BRB induced a significant 1.3-fold increase in the retinal transport of [^{3}H]-clonidine (Figure 3A).

Influence of sodium, potassium and chloride on [^{3}H]-clonidine BRB transport. We perfused the mouse eye with [^{3}H]-clonidine in Na^+-free/low carbonate buffers (lithium, NMDG-Cl, potassium and mannitol) at pH_e 7.40 and compared the transport parameters with those obtained after perfusion with [^{3}H]-clonidine in regular Krebs carbonate fluid (control; pH_e 7.40; Figure 3C). Perfusion of [^{3}H]-clonidine in these selected Na^+-free buffers (e.g. lithium, NMDG-Cl) produced no significant change in [^{3}H]-clonidine BRB transport (Figure 3C). Thus, sodium does not seem to be required for [^{3}H]-clonidine transport. The 'mannitol' carbonate perfusion fluid lacked Na^+ and contained only 3 mmol·L^{-1} Cl^-, unlike the other Na^+-free buffers (lithium, NMDG-Cl), which contained 130 mmol·L^{-1} Cl^-. A high K^+ extracellular content dissipates the *trans*-membrane potential gradient, and this could affect simple diffusion and/or carrier-mediated potential-sensitive transport components, so decreasing the transport of cationic compounds into depolarized cells. The high K^+ perfusion fluid (154 mmol·L^{-1}) did not altered [^{3}H]-clonidine transport (Figure 3C). The [^{3}H]-clonidine eye K_{in} transport when it was perfused in Krebs carbonate buffer (pH_e 7.40) in which chloride was replaced by gluconate and nitrate was not

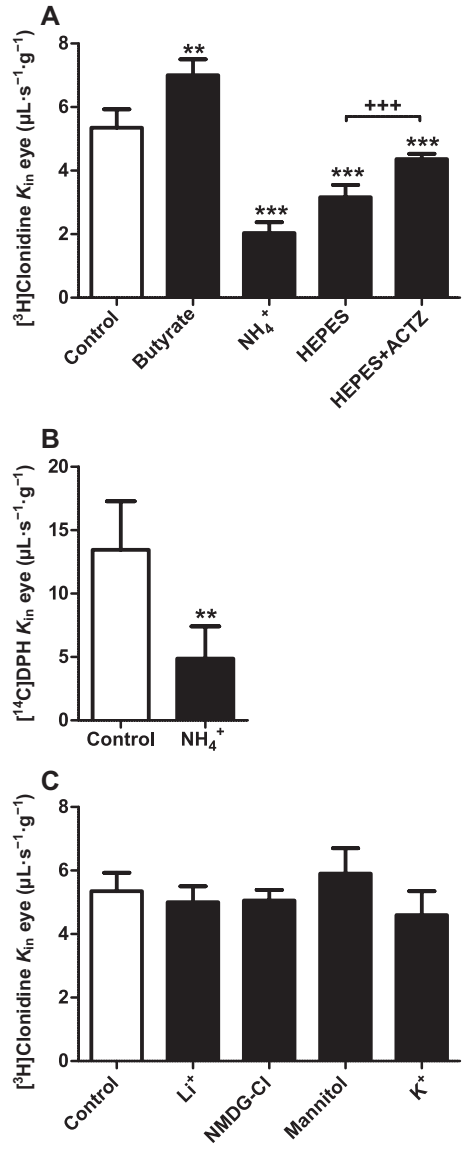

Figure 3

Effects of sodium, potassium and vascular perfusion fluids that could interfere with the regulation of the intracellular pH_i at the BRB. Control groups were always perfused with regular Krebs carbonate buffer. The perfusion fluids were at pH_e 7.40, and the transport of [^{3}H]-clonidine or [^{14}C]-DPH in the mouse eye (K_{in}; µL·s^{-1}·g^{-1}) was measured by *in situ* carotid perfusion for 120 and 60 s respectively. (A) Effects of altering pH_i on [^{3}H]-clonidine BRB transport. The vascular perfusion fluids were Krebs carbonate buffer with NH_4Cl (30 mmol·L^{-1}; 'NH_4^+'), Krebs carbonate with butyrate (100 mmol·L^{-1}), and HEPES-buffered fluid without or with acetazolamide (ACTZ; 10 mmol·L^{-1}). Data indicate means ± SD of 5–7 animals except in 'NH_4^+' experiments (n = 4). **P < 0.01, ***P < 0.001 compared with the control group. +++P < 0.001 compared with the same perfusion fluids with or without added ACTZ (10 mmol·L^{-1}). (B) Effect of altering pH_i on [^{14}C]-DPH BRB transport. The vascular perfusion fluid was Krebs carbonate buffer with NH_4Cl (30 mmol·L^{-1}; 'NH_4^+'). Data represent means ± SD (n = 4–6 mice). **P < 0.001 for comparisons between perfusion with and without NH_4Cl. (C) Effects of Na^+-free carbonate perfusion fluids (pH_e 7.40). Sodium was replaced by potassium (K^+, 154 mmol·L^{-1}), lithium (Li^+), N-methyl D-glucamine chloride (NMDG-Cl) or mannitol. Data represent means ± SD of 5–7 mice except 'Li^+' (n = 4).

significantly different from that obtained with control mice perfused with regular Krebs carbonate fluid for 120 s (pH_e 7.40; data not shown).

Brain transport of [^{3}H]-clonidine in selected transport-deficient and wild-type mouse (WT) strains

We assessed the effects of P-gp (Abcb1a) and Bcrp (Abcg2) on [^{3}H]-clonidine eye transport by perfusing control Fvb mice, TKO (Abcb1a$^{-/-}$, Abcb1b$^{-/-}$, Abcg2$^{-/-}$) Fvb mice and co-perfusion of elacridar (5 µmol·L^{-1}) in Swiss mice. The rates of [^{3}H]-clonidine retina transport in control WT mice (100 ± 11%), in TKO (Abcb1a$^{-/-}$, Abcb1b$^{-/-}$, Abcg2$^{-/-}$) mice (98 ± 4%; n = 4), and in mice perfused with fluid containing elacridar (96 ± 14%; n = 4) were not statistically different. The transport of [^{3}H]-clonidine in WT Fvb did not differ significantly from that in (Oct1$^{-/-}$, Oct2$^{-/-}$) mice (90 ± 15%; n = 4) or Oct3$^{-/-}$ mice (106 ± 8%; n = 5).

Effect of cis-inhibition of selected organic compounds on [^{3}H]-clonidine and [^{14}C]-DPH transport at the BRB

We carried out *cis*-inhibition experiments on the retina transport to discriminate between the involvements of known transporters and to obtain a molecular profile of the drugs interacting with the transporter. The concentrations were selected to obtain a modulation rather than to reflect the relevance of *in vivo* drug-drug interaction, as these unbound concentrations cannot be produced by systemic administration. Mice were perfused with Krebs carbonate buffer (pH_e 7.40) with [^{3}H]-clonidine (Tables 1 and 2) or [^{14}C]-DPH. Some of the compounds used (Table 1) are known to affect molecularly identified transporters handling some organic cations like OCT, OCTN and MATE; but those are ineffective in inhibiting this proton-antiporter (Chapy *et al.*, 2015). We used the characteristics of [^{3}H]-clonidine transport inhibitors to better identify the function of the transporter involved. Compounds like choline, tetraethylammonium (TEA), guanidine, agmatine, ergothioneine and carnitine did not significantly affect [^{3}H]-clonidine transport. Similarly, biogenic amines like dopamine, histamine and 5-HT were all without significant effect. However some cationic drugs showed a potency to inhibit [^{3}H]-clonidine BRB transport (Table 2). Psychoactive drugs such as opioids, amphetamines, tricyclic antidepressants or DPH inhibited significantly [^{3}H]-clonidine BRB transport. Antimalarial compounds and antiarrhythmic drugs (quinidine, verapamil) also had a significant inhibitory effect. The addition of an N-methyl moiety to naloxone decreased its ability to inhibit the transporter (Table 2). In the same way, the addition of a hydroxyl moiety to tryptamine (e.g. 5-HT) abolished its capacity to inhibit the transporter (Tables 1 and 2).

Mice were perfused for 60 s with [^{14}C]-DPH in Krebs carbonate buffer (pH_e 7.40) without or with clonidine (5 mmol·L^{-1}) or oxycodone (5 mmol·L^{-1}). The transport rate of [^{14}C]-DPH in the control group (100 ± 19%; n = 5) was significantly different (P < 0.01) from groups with clonidine (5 mmol·L^{-1}; 41 ± 16%; n = 5) and oxycodone (5 mmol·L^{-1}; 43 ± 15%; n = 5) co-perfusion.

Table 1

Effects of selected compounds on [^{3}H]-clonidine transport at the mouse BRB

Compound	Concentration (mmol·L^{-1})	Relative transport rate (% of control)
Agmatine	10	107 ± 21
L-carnitine	15	103 ± 28
Choline	10	95 ± 13
Corticosterone	0.01	105 ± 10
Dopamine	10	95 ± 20
L-DOPA	10	102 ± 11
Ergothioneine	1	107 ± 16
Guanidine	20	90 ± 15
Histamine	10	98 ± 12
5-HT	10	110 ± 10
Tetraethylammonium	15	115 ± 27

Cis-inhibition of [^{3}H]-clonidine (9 nmol·L^{-1}) transport at the BRB by unlabelled compounds was evaluated by *in situ* mouse carotid perfusion with Krebs carbonate perfusion fluid (pH$_e$ 7.40) for 120 s. BRB transport (K_{in}) in controls was 5.10 µL·s^{-1}·g^{-1} (100%). Data represent means ± SD (n = 5–6 mice, except for 'L-DOPA' and 'corticosterone' n = 4 mice).

Effect of trans-stimulation of selected drugs and compounds on [^{3}H]-clonidine BRB transport

The *trans*-stimulation technique provides a qualitative indication of whether a given compound is a substrate, but does not provide kinetic information to quantify active versus passive transport rate. We assessed the ability of some compounds present in the vascular compartment to further stimulate the exit of the accumulated [^{3}H]-clonidine at mouse BRB that could occur with a bidirectional transporter. The *trans*-efflux zero or exit of [^{3}H]-clonidine was stimulated by clonidine and by several compounds like DPH, verapamil, methadone, oxycodone, heroin, nicotine, MDMA and cocaine (Figure 4), suggesting that they may also be common substrates of the clonidine transporter. But an insignificant *trans*-stimulation provides no conclusive evidence that the tested compound is not a substrate. The *trans*-stimulation study also suggests that the transporter is bidirectional.

Discussion and conclusions

Many efforts have been made to predict the permeability of barriers to drugs using physicochemical descriptors, based on the assumption that drugs cross membranes only by passive diffusion. Clonidine a 'hydrophilic' drug exhibiting CNS activity has been considered an exception in this general assumption (Seelig *et al.*, 1994). However, we show here that

Table 2

Effects of selected compounds and cationic drugs on [^{3}H]-clonidine transport at the mouse BRB

Compound	Concentration (mmol·L^{-1})	Relative transport rate (% of control)
Psychostimulants		
p-Chloroamphetamine	10	29 ± 5***
Cocaine	10	34 ± 3***
Ecstasy (MDMA)	10	40 ± 6***
Nicotine	10	44 ± 12***
Tryptamine$^+$	10	44 ± 9***
Opioids		
Codeine	10	55 ± 16***
Heroin (diacetylmorphine)	10	34 ± 9***
Methadone	10	37 ± 4***
Morphine	10	67 ± 12**
Nalbuphine	10	43 ± 6***
Naloxone	3	73 ± 14*
	5	45 ± 11***
N-methyl naloxone	3	102 ± 14
Oxycodone	10	43 ± 4***
Tramadol	10	40 ± 4***
Antidepressants		
Desipramine	1	53 ± 8***
	10	32 ± 8***
Imipramine	1	27 ± 2***
Paroxetine	1	40 ± 1***
Antihistamines		
Diphenhydramine	1	58 ± 5***
	10	30 ± 4***
Antiemetic		
Alizapride	10	54 ± 9***
Antimalarials		
Amodiaquine	0.5	32 ± 5***
Quinine	10	37 ± 6***
Antiarrhythmics		
Quinidine	1	61 ± 3***
	10	33 ± 3***
Verapamil	1	55 ± 12***

Cis-inhibition of the BRB transport of [^{3}H]-clonidine (9 nmol·L^{-1}) by unlabelled compounds was evaluated by *in situ* mouse carotid perfusion with Krebs carbonate perfusion fluid (pH$_e$ 7.40) for 120 s. BRB transport (K_{in}) for controls was 5.10 µL·s^{-1}·g^{-1} (100%). Data represent means ± SD (n = 4–6 mice). *P < 0.05, **P < 0.01, ***P < 0.001 compared with control values. $^+$Endogenous compound.

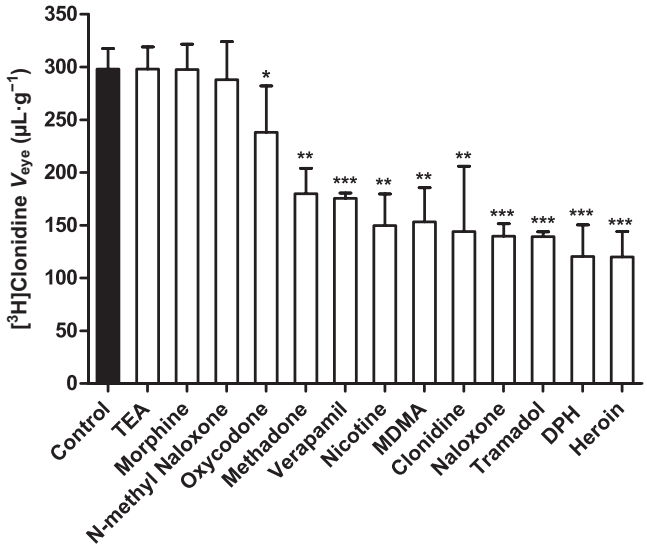

Figure 4

Trans-stimulation of [^{3}H]-clonidine in the eye. [^{3}H]-clonidine distribution volume at the BRB (V_{eye}; µL·g^{-1}) measured after *in situ* mouse carotid perfusion with Krebs carbonate buffer (pH_e 7.40) for 120 s, followed by a 60 s wash-out perfusion without [^{3}H]-clonidine. The last 60 s perfusion was at pH_e 6.40 without (Control) or with the unlabelled test compound, 10 mmol·L^{-1}, except for clonidine (1 mmol·L^{-1}), and verapamil (1 mmol·L^{-1}). Data are means ± SD of 5–7 mice except for 'MDMA', 'DPH' and 'clonidine' (n = 4). *P < 0.05, **P < 0.01, ***P < 0.001 compared with the control group.

the transport of the cationic drug clonidine at the mouse BRB as well as the transport of DPH combines both passive and carrier-mediated diffusion. The carrier-mediated system improves the transport of clonidine and DPH at the BRB by ~2.1- and 12.1-fold, respectively, compared with the passive diffusion rate at their vascular pharmacological concentration range. The evidence for a saturable clonidine or DPH influx highlights the critical role played by this transporter at the luminal/vascular membrane side of the mouse BRB.

Goldberg *et al.* (1987) demonstrated for the first time, *in vivo*, the role of a DPH uptake mechanism at the BBB by *in situ* rat brain perfusion experiments. Early studies in rats and at the sheep BBB provided no information regarding the molecular and/or functional identity of this transporter (Goldberg *et al.*, 1987; Au-Yeung *et al.*, 2006). However, recent advances and the discovery of SLC transporters such as OCT1-3 (SLC22A1-3), OCTN1-2 (SLC22A4-5) and MATE1 (SLC47A1) have improved our comprehension of the molecular mechanisms involved in cationic drug distribution in tissues (Roth *et al.*, 2012). To determine the involvement of these known cationic transporters, we used various strategies based on the modulation of drug transport using inorganic and organic chemicals, and drug transport in mice KO for the Oct1-3 transporters. Clonidine transport was clearly distinguished by its resistance to inhibition by TEA, a prototypical substrate/inhibitor of OCT, OCTN and MATE transporters. This was also confirmed by our studies with Oct-deficient mice. OCTN1 and MATE transporters are known to be proton-antiporters, but the lack of an effect of known inhibitors of these transporters (Table 1) argues against their involvement and suggests that clonidine transport at the BRB is mediated by a distinct but unknown sodium-independent proton-antiporter that is moreover insensitive to the *trans*-membrane potential, as demonstrated *in vivo* at the mouse BBB (Andre *et al.*, 2009).

Sampling the retina cannot kinetically determine whether the point of entry of a compound is the oBRB alone or the oBRB and iBRB (Newman, 2013; H. Chapy *et al.*, submitted). Although we can only speculate about the involvement of one or both BRB, the lack of pH_i changes in the absence of sodium, and the effects of butyrate or CA on pH_i modulation at the RPE are in agreement with a proton-antiporter function at least at the oBRB (Lin *et al.*, 1992; Kenyon *et al.*, 1997). Previous *in vitro* studies have evidenced a proton-antiporter implicated in the transport of clonidine and brimonidine (a clonidine-related drug) in a rat iBRB cell line and in human ARPE-19/oBRB cells, respectively (Zhang *et al.*, 2006; Kubo *et al.*, 2014), suggesting that the clonidine/proton-antiporter could be functional at both the iBRB and oBRB.

DPH transport also involves a proton-antiporter in Caco-2 cells (Mizuuchi *et al.*, 2000), and rat BBB cell line (Sadiq *et al.*, 2011), and additionally shares the MDMA/proton antiporter in Caco-2 cells (Kuwayama *et al.*, 2008). Our *trans*-stimulation studies at the mouse BRB have revealed bidirectional clonidine transport and suggested that several drugs, including DPH are also common substrates. The clonidine/proton- and DPH/proton-antiporters at the BRB are a single entity, as suggested by our *trans*-stimulation experiments, and as shown at the mouse BBB (Andre *et al.*, 2009). In addition to its similar K_m values at the mouse BRB and BBB (Andre *et al.*, 2009), the clonidine/proton-antiporter also displays similar biochemical features and inhibition profiles at the two sites, reinforcing the hypothesis of a single transporter entity at the two barriers. The relatively wide range of K_m values reported for substrates in the mouse, from 0.6 mM (clonidine) and 2.4 mM (nicotine) to ~4.5 mM (cocaine, DPH) (Andre *et al.*, 2009; Cisternino *et al.*, 2013; Chapy *et al.*, 2014), does not rule out the hypothesis of a single transporter entity. The apparent K_m of a transporter is a function of diverse molecular features (e.g. membrane permeation, binding, translocation and dissociation), unlike that of receptors/enzymes where substrate binding is the only event that occurs, and the K_m measured is only related to affinity. Indeed, functional studies support this diversity of substrate K_m values for transporters, such as in the case of GLUT1/SLC2A1 (1–20 mmol·L^{-1}) and P-gp (Rumsey *et al.*, 1997; Cisternino *et al.*, 2004; Augustin, 2010). According to the K_m and V_{max} values reported *in vivo* in the mouse and the usual pharmacological concentrations of their substrates, this transporter can be described as a 'low-affinity', high-capacity system that efficiently transports substrates and is unlikely to lead to drug–drug interactions. The unbound plasma concentrations of clonidine or DPH will never exceed their K_m. This property allows the transport of substrates without the risk of drug saturation (i.e. a non-linear process) whatever their unbound vascular concentration.

The involvement of a proton-antiporter in the handling of several cationic drugs such as nicotine, tramadol, MDMA and cocaine has been already evidenced at the mouse BBB (Cisternino *et al.*, 2013; Chapy *et al.*, 2014) as well as in

diverse human and/or rodent BBB cell lines (Kuwayama *et al*., 2008; Okura *et al*., 2008; Chapy *et al*., 2014; Kitamura *et al*., 2014). The experiments presented here imply that this carrier-mediated mechanism is also involved at the BRB for these drugs. Although oxycodone and naloxone, whose molecular structures are related to morphine, have been shown to be carried by a proton-antiporter at the BBB (Okura *et al*., 2008; Chapy *et al*., 2015), our *trans*-stimulation experiments fail to prove that morphine and N-methyl naloxone are substrates of the clonidine transporter, which is actually in agreement with morphine low BBB permeability (Cisternino *et al*., 2004). The brain kinetics of methadone also suggests that its BBB permeability could primarily involve an influx process (Kalvass *et al*., 2007). Our results propose for the first time that methadone and heroin could also be substrates for this proton-antiporter, and that verapamil transport could also involve a proton-antiporter-mediated mechanism at the BRB and BBB, in agreement with other experiments specifically addressing this question (H. Chapy *et al*., submitted).

Our study also suggests that this proton-antiporter could be a critical factor in the PK-PD variability of clonidine and DPH at the retina. The pharmacological/toxicological effects of drugs depend on both their ability to permeate the tissue and to interact with pharmacological targets/receptors. Melanins, which are indole derivatives and regular targets of toxic drugs in the retina/oBRB, have been shown to interact with a wide range of basic/cationic drugs leading to retinal toxicity (Zane *et al*., 1990; King *et al*., 2009). However, the ability of toxic drugs to bind to retinal melanin has not been found to be predictive of their ocular toxicity (Leblanc *et al*., 1998). Although the actual picture of many drugs is governed by their consistent ability to passively diffuse across any barrier and to be distributed throughout the body, the involvement of a transporter handling several basic/cationic drugs at the oBRB could represent a critical determinant in the RPE-specific intracellular accumulation of substrates, favouring interactions with melanins. A physiological substrate for this proton-antiporter remains to be determined but interestingly, tryptamine, an endogenous indole derivative, interacts with it at least as an inhibitor, unlike dopamine, L-DOPA and 5-HT, which are also possibly involved in melanin pathways (Bush *et al*., 2006). The ability of some antimalarial drugs like amodiaquine and quinine, quinidine and tricyclic antidepressants (e.g. desipramine and imipramine), which are all also known to induce melanin/retinal toxicity, to interact with or inhibit the proton-antiporter could represent further leads to explore. An effective drug inhibitor that could reach unbound concentrations high enough to lead to drug interactions *in vivo* after systemic administration is yet unknown. However, these inferences still need to be confirmed for endogenous substrate(s).

In conclusion, the feature of this molecularly unknown sodium-independent and *trans*-membrane potential-insensitive clonidine-and-DPH/proton-antiporter highlights its importance in regulating DPH and clonidine delivery to the retina, and is a new element that must be taken into consideration for PK prediction and in the analysis of the pharmacotoxicological variability of exposure to the drugs. Our experiments suggest that this transporter has the capacity to handle several drugs such as methadone, heroin and verapamil. The demonstration of this second *in vivo* physiological localization at the BRB suggests the existence of a common endogenous substrate in both the brain and the retina whose functions remain to be determined, and extend the potential of this transporter as a new target and strategy to improve drug delivery into the brain and the retina.

Acknowledgements

We thank Dr. Alfred H. Schinkel for supplying the KO mice, GSK for generously supplying elacridar and Prof. H. Galons for generously supplying MDMA. We thank Dr S. Rasika for editing the English text. We also thank the Paris Descartes University foundation and Servier Laboratories for the financial support granted to Hélène Chapy. Salvatore Cisternino received a grant from the University Paris Descartes – Sorbonne Paris Cité (appel d'offres 2012: projets de recherche collaboratifs intersites).

Author contributions

H. C., P. A., X. D., J.M. S. and S. C. designed the research study and approved the Ms. H. C., P. A. and S. C. performed the research. H. C., P. A. and S. C. analysed the data. H. C. and S. C. wrote the paper.

Conflict of interest

None.

References

Abbott NJ, Patabendige AA, Dolman DE, Yusof SR, Begley DJ (2010). Structure and function of the blood-brain barrier. Neurobiol Dis 37: 13–25.

Alexander SPH, Benson HE, Faccenda E, Pawson AJ, Sharman JL, Spedding M *et al.* (2013). The concise guide to pharmacology 2013/14: transporters. Br J Pharmacol 170: 1706–1796.

Andre P, Debray M, Scherrmann JM, Cisternino S (2009). Clonidine transport at the mouse blood-brain barrier by a new H+ antiporter that interacts with addictive drugs. J Cereb Blood Flow Metab 29: 1293–1304.

Andre P, Saubamea B, Cochois-Guegan V, Marie-Claire C, Cattelotte J, Smirnova M *et al.* (2012). Transport of biogenic amine neurotransmitters at the mouse blood-retina and blood-brain barriers by uptake1 and uptake2. J Cereb Blood Flow Metab 32: 1989–2001.

Au-Yeung SC, Rurak DW, Gruber N, Riggs KW (2006). A pharmacokinetic study of diphenhydramine transport across the blood-brain barrier in adult sheep: potential involvement of a carrier-mediated mechanism. Drug Metab Dispos 34: 955–960.

Augustin R (2010). The protein family of glucose transport facilitators: It's not only about glucose after all. IUBMB Life 62: 315–333.

Bush WD, Garguilo J, Zucca FA, Albertini A, Zecca L, Edwards GS *et al*. (2006). The surface oxidation potential of human neuromelanin reveals a spherical architecture with a pheomelanin core and a eumelanin surface. Proc Natl Acad Sci U S A 103: 14785–14789.

Cattelotte J, Andre P, Ouellet M, Bourasset F, Scherrmann JM, Cisternino S (2008). In situ mouse carotid perfusion model: glucose and cholesterol transport in the eye and brain. J Cereb Blood Flow Metab 28: 1449–1459.

Chapy H, Smirnova M, Andre P, Schlatter J, Chiadmi F, Couraud PO *et al*. (2014). Carrier-mediated cocaine transport at the blood-brain barrier as a putative mechanism in addiction liability. Int J Neuropsychopharmacol 18. doi:10.1093/ijnp/pyu001.

Chapy H, Goracci L, Vayer P, Parmentier Y, Carrupt PA, Decleves X *et al*. (2015). Pharmacophore-based discovery of inhibitors of a novel drug proton-antiporter in human brain endothelial hCMEC/D3 cell line. Br J Pharmacol. doi:10.1111/bph.13258.

Cisternino S, Rousselle C, Debray M, Scherrmann JM (2004). In situ transport of vinblastine and selected P-glycoprotein substrates: implications for drug-drug interactions at the mouse blood-brain barrier. Pharm Res 21: 1382–1389.

Cisternino S, Chapy H, Andre P, Smirnova M, Debray M, Scherrmann JM (2013). Coexistence of passive and proton antiporter-mediated processes in nicotine transport at the mouse blood-brain barrier. AAPS J 15: 299–307.

Crassous PA, Denis C, Paris H, Senard JM (2007). Interest of alpha2-adrenergic agonists and antagonists in clinical practice: background, facts and perspectives. Curr Top Med Chem 7: 187–194.

Fischer W, Metzner L, Hoffmann K, Neubert RH, Brandsch M (2006). Substrate specificity and mechanism of the intestinal clonidine uptake by Caco-2 cells. Pharm Res 23: 131–137.

Giacomini KM, Consortium IT, Huang SM, Tweedie DJ, Benet LZ, Brouwer KL *et al*. (2010). Membrane transporters in drug development. Nat Rev Drug Discov 9: 215–236.

Goldberg MJ, Spector R, Chiang CK (1987). Transport of diphenhydramine in the central nervous system. J Pharmacol Exp Ther 240: 717–722.

Han YH, Sweet DH, Hu DN, Pritchard JB (2001). Characterization of a novel cationic drug transporter in human retinal pigment epithelial cells. J Pharmacol Exp Ther 296: 450–457.

Kalvass JC, Maurer TS, Pollack GM (2007). Use of plasma and brain unbound fractions to assess the extent of brain distribution of 34 drugs: comparison of unbound concentration ratios to in vivo p-glycoprotein efflux ratios. Drug Metab Dispos 35: 660–666.

Kell DB, Dobson PD, Bilsland E, Oliver SG (2013). The promiscuous binding of pharmaceutical drugs and their transporter-mediated uptake into cells: what we (need to) know and how we can do so. Drug Discov Today 18: 218–239.

Kenyon E, Maminishkis A, Joseph DP, Miller SS (1997). Apical and basolateral membrane mechanisms that regulate pHi in bovine retinal pigment epithelium. Am J Physiol 273 (2 Pt 1): C456–C472.

Kilkenny C, Browne W, Cuthill IC, Emerson M, Altman DG (2010). Animal research: Reporting *in vivo* experiments: the ARRIVE guidelines. Br J Pharmacol 160: 1577–1579.

King G, Yerger VB, Whembolua GL, Bendel RB, Kittles R, Moolchan ET (2009). Link between facultative melanin and tobacco use among African Americans. Pharmacol Biochem Behav 92: 589–596.

Kitamura A, Higuchi K, Okura T, Deguchi Y (2014). Transport characteristics of tramadol in the blood-brain barrier. J Pharm Sci 103: 3335–3341.

Kubo Y, Tsuchiyama A, Shimizu Y, Akanuma SI, Hosoya KI (2014). Involvement of carrier-mediated transport in the retinal uptake of clonidine at the inner blood-retinal barrier. Mol Pharm 11: 3747–3753.

Kuwayama K, Inoue H, Kanamori T, Tsujikawa K, Miyaguchi H, Iwata Y *et al*. (2008). Uptake of 3,4-methylenedioxymethamphetamine and its related compounds by a proton-coupled transport system in Caco-2 cells. Biochim Biophys Acta 1778: 42–50.

Leblanc B, Jezequel S, Davies T, Hanton G, Taradach C (1998). Binding of drugs to eye melanin is not predictive of ocular toxicity. Regul Toxicol Pharmacol 28: 124–132.

Lin H, Kenyon E, Miller SS (1992). Na-dependent pHi regulatory mechanisms in native human retinal pigment epithelium. Invest Ophthalmol Vis Sci 33: 3528–3538.

McGrath J, Drummond G, McLachlan E, Kilkenny C, Wainwright C (2010). Guidelines for reporting experiments involving animals: the ARRIVE guidelines. Br J Pharmacol 160: 1573–1576.

Mizuuchi H, Katsura T, Ashida K, Hashimoto Y, Inui K (2000). Diphenhydramine transport by pH-dependent tertiary amine transport system in Caco-2 cells. Am J Physiol Gastrointest Liver Physiol 278: G563–G569.

Newman EA (2013). Functional hyperemia and mechanisms of neurovascular coupling in the retinal vasculature. J Cereb Blood Flow Metab 33: 1685–1695.

Ochrietor JD, Clamp MF, Moroz TP, Grubb JH, Shah GN, Waheed A *et al*. (2005). Carbonic anhydrase XIV identified as the membrane CA in mouse retina: strong expression in Müller cells and the RPE. Exp Eye Res 81: 492–500.

Okura T, Hattori A, Takano Y, Sato T, Hammarlund-Udenaes M, Terasaki T *et al*. (2008). Involvement of the pyrilamine transporter, a putative organic cation transporter, in blood-brain barrier transport of oxycodone. Drug Metab Dispos 36: 2005–2013.

Pawson AJ, Sharman JL, Benson HE, Faccenda E, Alexander SP, Buneman OP *et al*.; NC-IUPHAR. (2014) The IUPHAR/BPS Guide to PHARMACOLOGY: an expert-driven knowledgebase of drug targets and their ligands. Nucl Acids Res 42 (Database Issue): D1098–D1106.

Pomerleau AC, Gooden CE, Fantz CR, Morgan BW (2014). Dermal exposure to a compounded pain cream resulting in severely elevated clonidine concentration. J Med Toxicol 10: 61–64.

Pragst F, Herre S, Bakdash A (2006). Poisonings with diphenhydramine–a survey of 68 clinical and 55 death cases. Forensic Sci Int 161: 189–197.

Ronaldson PT, Davis TP (2013). Targeted drug delivery to treat pain and cerebral hypoxia. Pharmacol Rev 65: 291–314.

Roth M, Obaidat A, Hagenbuch B (2012). OATPs, OATs and OCTs: the organic anion and cation transporters of the SLCO and SLC22A gene superfamilies. Br J Pharmacol 165: 1260–1287.

Rumsey SC, Kwon O, Xu GW, Burant CF, Simpson I, Levine M (1997). Glucose transporter isoforms GLUT1 and GLUT3 transport dehydroascorbic acid. J Biol Chem 272: 18982–18989.

Sadiq MW, Borgs A, Okura T, Shimomura K, Kato S, Deguchi Y *et al*. (2011). Diphenhydramine active uptake at the blood-brain barrier and its interaction with oxycodone in vitro and in vivo. J Pharm Sci 100: 3912–3923.

Seelig A, Gottschlich R, Devant RM (1994). A method to determine the ability of drugs to diffuse through the blood-brain barrier. Proc Natl Acad Sci U S A 91: 68–72.

Takasato Y, Rapoport SI, Smith QR (1984). An in situ brain perfusion technique to study cerebrovascular transport in the rat. Am J Physiol 247 (3 Pt 2): H484–H493.

Taylor CJ, Nicola PA, Wang S, Barrand MA, Hladky SB (2006). Transporters involved in regulation of intracellular pH in primary cultured rat brain endothelial cells. J Physiol 576 (Pt 3): 769–785.

Zane PA, Brindle SD, Gause DO, O'Buck AJ, Raghavan PR, Tripp SL (1990). Physicochemical factors associated with binding and retention of compounds in ocular melanin of rats: correlations using data from whole-body autoradiography and molecular modeling for multiple linear regression analyses. Pharm Res 7: 935–941.

Zhang N, Kannan R, Okamoto CT, Ryan SJ, Lee VH, Hinton DR (2006). Characterization of brimonidine transport in retinal pigment epithelium. Invest Ophthalmol Vis Sci 47: 287–294.